



ChemComm

**CAAC–IPr*: Easily Accessible, Highly Sterically-Hindered
Cyclic (Alkyl)(Amino)Carbenes**

Journal:	<i>ChemComm</i>
Manuscript ID	CC-COM-10-2022-005668.R1
Article Type:	Communication

SCHOLARONE™
Manuscripts

COMMUNICATION

CAAC–IPr*: Easily Accessible, Highly Sterically-Hindered Cyclic (Alkyl)(Amino)Carbenes

Wenchao Chu,^a Tongliang Zhou,^a Elwira Bisz,^b Błażej Dziuk,^c Roger Lalancette,^a Roman Szostak,^d and Michal Szostak^{*,a}

Received 00th January 20xx,
Accepted 00th January 20xx

DOI: 10.1039/x0xx00000x

IPr* (IPr* = 1,3-bis(2,6-bis(diphenylmethyl)-4-methylphenyl)imidazol-2-ylidene) has emerged as a powerful highly hindered and sterically-flexible ligand platform for transition-metal catalysis. CAACs (CAAC = cyclic (alkyl)(amino)carbenes) have gained major attention as strongly electron-rich carbon analogues of NHCs (NHC = N-heterocyclic carbene) with broad applications in both industry and academia. Herein, we report a merger of CAAC ligands with highly-hindered IPr*. The efficient synthesis, electronic characterization and application in model Cu-catalyzed hydroboration of alkynes is described. The ligands are strongly electron-rich, bulky and flexible around the N-Ar wingtip. The availability of various IPr* and CAAC templates offers a significant potential to expand the existing arsenal of NHC ligands to electron-rich bulky architectures with critical applications in metal stabilization and catalysis.

The development of new catalysts represents one of the most fundamental approaches to advance the field of organic synthesis.^{1,2} In this context, the isolation of N-heterocyclic carbenes by Arduengo in 1991,³ quickly followed by extensive studies in catalysis by Herrmann and the introduction of IPr as the privileged ligand by the Nolan group (IPr = 1,3-bis(2,6-diisopropylphenyl)imidazol-2-ylidene) have launched expansive research on N-heterocyclic carbenes (Figure 1).^{4,5} At present, NHC ligands have found ubiquitous applications in catalysis, materials science, energy research and medicinal chemistry, where the imidazole scaffold provides numerous avenues to tune the properties of the organometallic system.⁶ In 2005, the Bertrand group discovered that σ -donation of NHCs can be significantly enhanced by replacing one of the nitrogen substituents with less electronegative quaternary carbon atom in CAAC ligands.⁷ The presence of sp^3 -hybridized carbon instead of planar nitrogen further provides sterically-differentiated

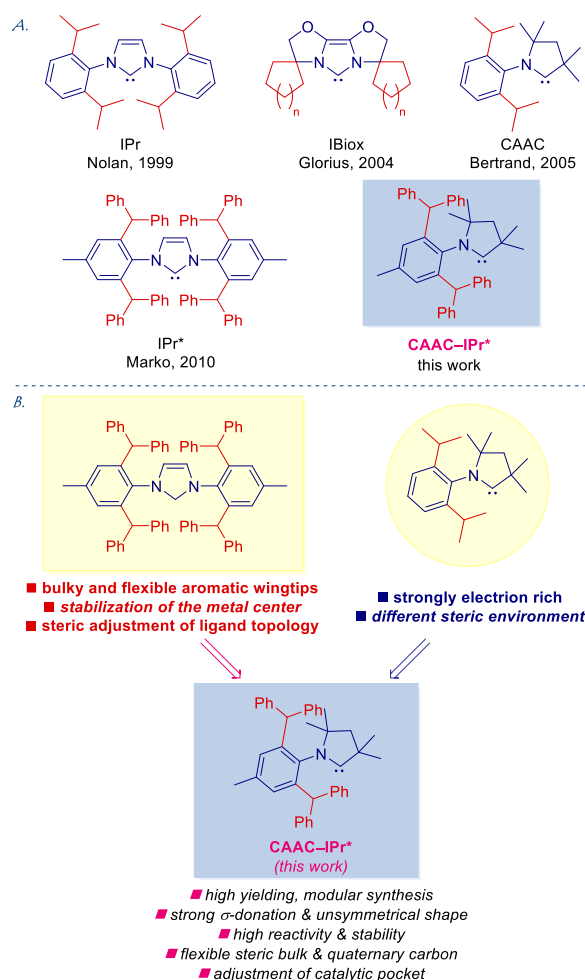


Figure 1. Sterically-demanding N-heterocyclic carbenes.

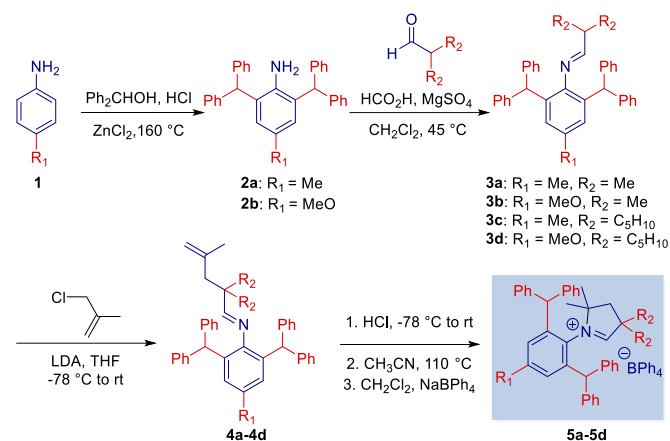
environment around the metal center,⁸ making CAACs broadly popular ligands in various areas of catalysis and main metal chemistry in both academic and industrial settings.⁹ Simultaneously, IPr* ligands featuring bulky and flexible aromatic wingtips have emerged as a powerful platform in transition-metal catalysis (Figure 1).¹⁰ In these ligands, the

^a Department of Chemistry, Rutgers University, 73 Warren Street, Newark, New Jersey 07102, United States

^b Department of Chemistry, Opole University, 48 Oleska Street, Opole 45-052, Poland

^c Department of Chemistry, University of Science and Technology, Norwida 4/6, Wrocław 50-373, Poland

^d Department of Chemistry, Wrocław University, F. Joliot-Curie 14, Wrocław 50-383, Poland



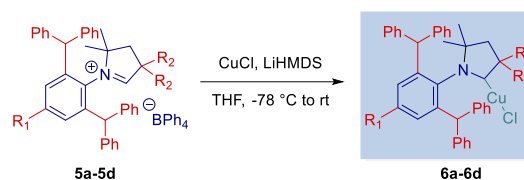
Scheme 1. Synthesis of CAAC-IPr* Salts. Conditions: (a) **1** (1.0 equiv), Ph₂CHOH (2 equiv), ZnCl₂ (0.5 equiv), HCl (36% aq., 1.0 equiv), 160 °C, 15 h. **2a**: 89%; **2b**: 92%. (b) **2** (1.0 equiv), RCHO (1.5 equiv), HCO₂H (0.05 equiv), MgSO₄ (5 equiv), CH₂Cl₂, 45 °C, 24 h. **3a**: 70%; **3b**: 73%; **3c**: 65%; **3d**: 61%. (c) **3** (1.0 equiv), LDA (3.6 equiv), 3-chloro-2-methylprop-1-ene (6 equiv), THF, -78 °C-rt, 20 h. **4a**: 85%; **4b**: 82%; **4c**: 75%; **4d**: 72%. (d) (i) HCl (2 M in Et₂O, 1.1 equiv), hexane, -78 °C-rt, 30 min; (ii) CH₃CN, 110 °C, 24 h; (iii) NaBPh₄ (5 equiv), CH₂Cl₂, rt, 15 h. **5a**: 65%; **5b**: 61%; **5c**: 71%; **5d**: 74%. See SI for details.

extremely bulky N-aromatic wingtips provide kinetic stabilization of the metal center, while the flexibility rendered by benzhydryl substituents enables steric adjustments of the ligand topology. At present, IPr* and counterparts are among the successful successors to IPr in the rapidly growing area of N-heterocyclic carbenes.

Inspired by the elegant studies in NHC ligand development by the groups of Nolan,¹¹ Bertrand,^{7,9,12} Glorius,¹³ Marko¹⁴ and others,^{6,8,15} and following our interest in NHC ligands in catalysis,¹⁶ we considered a merger of sterically-hindered IPr* and strongly electron-rich CAAC ligands (Figure 1B). We hypothesized that this unique class of ligands would combine the properties of both families of ligands, while providing a new strategy for the development of electron-rich, flexible and extremely bulky catalyst architectures.

The synthesis of IPr*-CAAC^{Me} bearing methyl substituents at the quaternary carbon was selected as a starting point (Scheme 1, **5a**). After experimentation, we were pleased to find that a route involving condensation of 2,6-bis(diphenylmethyl)-4-toluidine with 2-methylpropanal and catalytic formic acid in CH₂Cl₂ at 45 °C afforded the product imine in 70% yield.^{16f} The subsequent α -alkylation was accomplished with excess of LDA and 3-chloro-2-methylprop-1-ene in 85% yield. Finally, the intramolecular cyclization proceeded in 65% yield to give IPr*-CAAC^{Me} as HBPh₄ salt by a sequence involving N-protonation with HCl at -78 °C to give alkenyl iminium, ring closure at 110 °C and counterion exchange with NaBPh₄ to facilitate purification.

It should be noted that condensation, alkylation and cyclization steps are significantly more challenging with the bulky IPr* aniline than with less hindered anilines, such as Dipp (Dipp = 2,6-diisopropylaniline) due to steric hindrance of benzhydryl substituents. The synthesis of more electron-rich analogue bearing 4-methoxy substitution at the N-Ar wingtip, IPr*^{MeO}-CAAC^{Me} (**5b**) as well as analogues bearing cyclohexyl moiety that provide “flexible wall” at the quaternary carbon, IPr*-CAAC^{Cy} (**5c**) and IPr*^{MeO}-CAAC^{Cy} (**5d**), was successfully



Scheme 2. Synthesis of [Cu(IPr*-CAAC)Cl] Complexes. Conditions: **5** (1 equiv), CuCl (3 equiv), LiHMDS (3 equiv), THF, -78 °C-rt, 20 h. **6a**: 82%; **6b**: 64%; **6c**: 87%; **6d**: 69%.

accomplished following the same procedures (Scheme 1), attesting to the generality of the approach.

With access to IPr*-CAAC^{Me} secured, we next evaluated complexation with CuCl. [Cu(IPr*-CAAC)Cl] complexes were selected as model systems due to the predicted linear geometry and the recent advances in the use of Cu-CAACs in catalysis.¹⁷ Complexes [Cu(IPr*-CAAC^{Me})Cl] (**6a**), [Cu(IPr*^{MeO}-CAAC^{Me})Cl] (**6b**), [Cu(IPr*-CAAC^{Cy})Cl] (**6c**), and [Cu(IPr*^{MeO}-CAAC^{Cy})Cl] (**6d**) were readily prepared by a deprotonation route with LiHMDS at -78 °C in 64–87% yields (Scheme 2). All complexes **6a–6d** were found to be stable to air and moisture. Complexes **6a** and **6b** were fully characterized by x-ray crystallography (Figure 2 and 3). Studies by Nolan and Cavallo demonstrated that % buried volume (%V_{bur}) and steric maps of linear NHC-metal complexes provide the best indication of steric impact of NHC ligands.¹⁸ [Cu(IPr*-CAAC^{Me})Cl] and [Cu(IPr*^{MeO}-CAAC^{Me})Cl] are linear (**6a**: C–Cu–Cl, 174.45°; C–Cu, 1.864 Å; **6b**: C–Cu–Cl, 176.06°; C–Cu, 1.882 Å), making them good models for evaluating %V_{bur}. With the (%V_{bur}) of 49.5% and 49.4%, [Cu(IPr*-CAAC^{Me})Cl] and [Cu(IPr*^{MeO}-CAAC^{Me})Cl] represent the bulkiest CAAC^{Me} ligands developed to date. These values can be compared with the (%V_{bur}) of 41.9% determined for [Cu(Dipp-CAAC^{Me})Cl] (C–Cu–Cl, 173.66°; C–Cu, 1.878 Å). Note that the (%V_{bur}) of [Cu(IPr*-CAAC^{Me})Cl] and [Cu(IPr*^{MeO}-CAAC^{Me})Cl] approaches the (%V_{bur}) determined for imidazol-2-ylidene [Cu(IPr*)Cl] of 52.1%.

The crystallographic analysis of [Cu(IPr*-CAAC^{Me})Cl] and [Cu(IPr*^{MeO}-CAAC^{Me})Cl] revealed spatially-distinct unsymmetrical quadrant distribution (Figure 3). The values indicate significant steric enhancement vs. [Cu(Dipp-CAAC^{Me})Cl] (SW 34%, NW 32.0%, NE 54.5%, SE 47.1%),¹⁷ and clearly distinguish the quaternary carbon-substituted unsymmetrical CAACs from their symmetrical imidazol-2-ylidene counterparts ([Cu(IPr*)Cl], SW 63.1%, NW 54.9%, NE 42.5%, SE 48.1%). This provides important differentiated steric quadrant distribution in combination with flexible-CHPh₂ aryl wingtip topology. Note that CAAC-IPr* are more sterically-bulky than IPr* (NE, SE quadrants, Figure 3), which clearly results from the presence of a quaternary center adjacent to the carbenic carbon.

We have further prepared selenourea adduct, [Se(IPr*-CAAC^{Me})] (**7**), to evaluate π -backbonding from the ⁷⁷Se spectra (Scheme 3). The δ_{se} value of 532.45 ppm (CDCl₃) for [Se(IPr*-CAAC^{Me})] can be compared with Dipp-CAAC^{Me} (δ_{se} = 492 ppm), indicating enhancement of π -backbonding, as expected from the 2,6-bis(benzhydryl) substitution (IPr*: δ_{se} = 106 ppm).¹⁹ Furthermore, one-bond CH *J* coupling constant gives a good indication of σ -donating properties (*vide infra*). The value of 181.67 Hz for IPr*-CAAC^{Me}HCl (DMSO-*d*₆) indicates this ligand as strongly σ -donating (IPr*: 223.70 Hz; Dipp-CAAC^{Cy}: 188.53 Hz),²⁰ while at the same time more sterically-demanding and flexible. The chemical shift of the iminium proton in IPr*-CAAC^{Me}HCl was found at 5.76 ppm (CDCl₃),

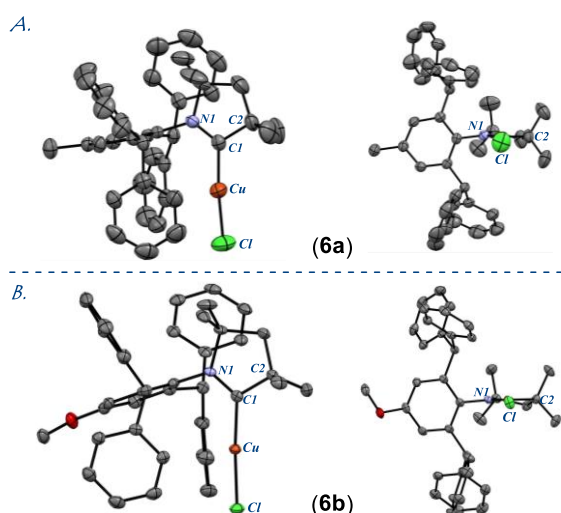


Figure 2. X-ray crystal structure of **6a–6b**. Two views: front (left); side (right). Hydrogen atoms have been omitted for clarity. Selected bond lengths [Å] and angles [°]: **6a**: Cu–C1, 2.0835(9); Cu–C1, 1.864(2); N1–C1, 1.300(3); N1–C9, 1.459(4); C1–C2, 1.512(4); C1–Cu–C1, 174.45(8); C1–N1–C4, 115.4(2); C1–N1–C9, 122.7(2); C4–N1–C9, 121.8(2); Cu–C1–C2, 122.4(2); Cu–C1–N1, 128.6(2); N1–C1–C2, 122.4(2). **6b**: Cu–C1, 2.1142(5); Cu–C1, 1.882(1); N1–C1, 1.305(2); N1–C9, 1.457(2); C1–C2, 1.519(2); C1–Cu–C1, 176.06(5); C1–N1–C4, 115.3(1); C1–N1–C9, 121.6(1); C4–N1–C9, 123.1(1); Cu–C1–C2, 122.5(1); Cu–C1–N1, 128.2(1); N1–C1–C2, 122.5(1). CCDC 2209831 (**6a**). CCDC 2209832 (**6b**).

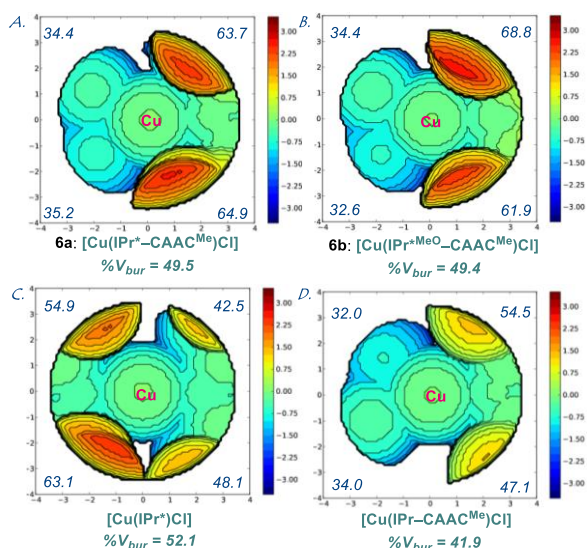
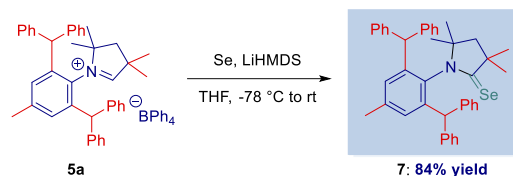


Figure 3. (A–D) Topographical steric maps of [Cu(IPr*–CAAC^{Me})Cl] **6a**, [Cu(IPr*MeO–CAAC^{Me})Cl] **6b**, [Cu(IPr*)Cl], [Cu(IPr*–CAAC^{Me})Cl] showing %V_{bur} per quadrant.

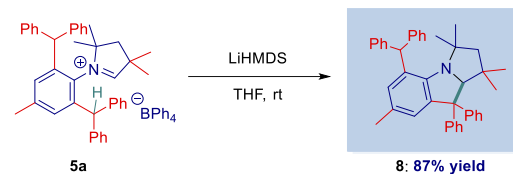
which is significantly upfield compared with imidazolium IPr* salt (13.0 ppm).¹⁴

Interestingly, we found that the carbene generated from IPr*–CAAC^{Me} undergoes intramolecular C–H activation at room temperature to afford benzopyrrolidine in excellent 87% yield (Scheme 4, **8**). This reaction is driven by the steric arrangement of the carbene in the close proximity to the benzylic C–H position, providing a unique access to biologically active pyrrolidine scaffolds.

The activity of [Cu(IPr*–CAAC)Cl] complexes was evaluated in Cu-catalyzed hydroboration of alkynes (Scheme 5). Recently, there have been major advances in Cu–CAAC-catalyzed borylcupration of alkynes, where Cu–CAACs have been identified to provide complementary regioselectivity to Cu–imidazol-2-ylidenes.¹⁷



Scheme 3. Synthesis of [Se(IPr*–CAAC^{Me})]

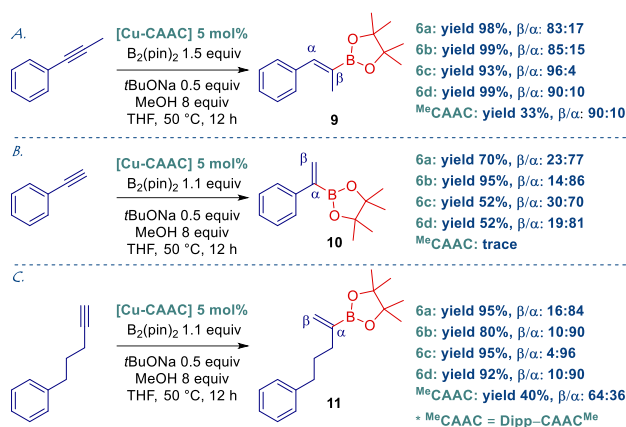


Scheme 4. Intramolecular C–H Activation

We selected this reaction as a model system vs. the parent CAAC^{Me}. All IPr*–CAAC catalysts were evaluated against the standard Dipp–CAAC^{Me} to gauge the effect of steric ligand substitution. As shown, IPr*–CAAC–Cu significantly improves the efficiency and regioselectivity of borylcupration cf. the parent CAAC^{Me}. In the hydroboration of 1-phenyl-1-propyne, the most effective is [Cu(IPr*–CAAC^{Cy})Cl] (**6c**) affording β-hydroboration product in 93% yield and 96:4 β-selectivity. All IPr*–CAAC–Cu catalysts significantly outperform the unhindered Dipp–CAAC^{Me}–Cu. In the hydroboration of phenylacetylene, the most effective is [Cu(IPr*MeO–CAAC^{Me})Cl] (**6b**), affording the hydroboration product in 95% yield and 86:14 α-selectivity, while other IPr*–CAAC–Cu catalysts provide good levels of efficiency (52–70% yields). Of note, Dipp–CAAC^{Me}–Cu is completely ineffective under these conditions. Finally, in hydroboration of pent-4-yn-1-ylbenzene, the most effective is [Cu(IPr*–CAAC^{Cy})Cl] (**6c**), affording the hydroboration product in 95% yield and 96:4 α-selectivity. Again, all IPr*–CAAC–Cu catalysts significantly outperform Dipp–CAAC^{Me}–Cu.

To gain insight into the electronic properties of IPr*–CAACs, HOMO and LUMO energy levels were determined at the B3LYP 6-311++g(d,p) level (Figure 4 and SI). Most importantly, the HOMO of IPr*–CAAC^{Me} (–5.49 eV) is significantly higher than IPr* (–6.01 eV), which is a model for σ-donating NHCs. This value can be compared with Dipp–CAAC^{Me} (–5.33 eV) and IPr* (–6.12 eV). Furthermore, the LUMO of IPr*–CAAC^{Me} (–0.90 eV) can be compared with Dipp–CAAC^{Me} (–5.33 eV) and IPr* (–6.12 eV). Furthermore, the LUMO of IPr*–CAAC^{Me} (–0.90 eV) can be compared with IPr* (–0.48 eV, LUMO+1 due to required symmetry), Dipp–CAAC^{Me} (–0.51 eV) and IPr* (–0.90 eV). Thus, the strong σ-donation of IPr*–CAACs in combination with variable bulk makes this class of NHCs well-suited for catalysis. Note the enhancement of π-acceptance of CAAC–IPr* as a result of ortho-benzhydryl substituents.^{16f} At this stage, we have been unable to determine TEP due to facile C–H activation.^{15,16f}

Furthermore, to eliminate impact from steric packing, the percent buried volume (%V_{bur}) was calculated from the optimized structures of [Cu(CAAC)Cl] complexes **6a–6d** at the B3LYP 6-311++g(d,p) level (see SI). These studies determined the %V_{bur} of NHC in [Cu(IPr*–CAAC^{Me})Cl] (**6a**) as 47.1% (SW, 31.8%; NW, 34.7%; NE, 62.3%; SE, 59.7%); [Cu(IPr*MeO–CAAC^{Me})Cl] (**6b**) as 47.1% (SW, 31.8%; NW, 35.0%; NE, 61.9%; SE, 59.6%); [Cu(IPr*–CAAC^{Cy})Cl] (**6c**) as 47.3% (SW, 32.1%; NW, 34.9%; NE, 62.5%; SE, 59.8%); and in [Cu(IPr*MeO–CAAC^{Cy})Cl] (**6d**) as 47.3% (SW, 32.1%; NW, 35.4%; NE, 62.0%; SE, 59.8%). The unsymmetrical geometry rendered by the quaternary carbon provides unique steric environment of these strongly σ-donating NHC ligands.



Scheme 5. Hydroboration of Alkynes Catalyzed by [Cu(IPr*-CAAC)Cl]. Catalyst (0.05 equiv), B₂Pin₂ (1.5 or 1.1 equiv), tBuONa (0.5 equiv), MeOH (8 equiv), THF, 50 °C, 12 h.

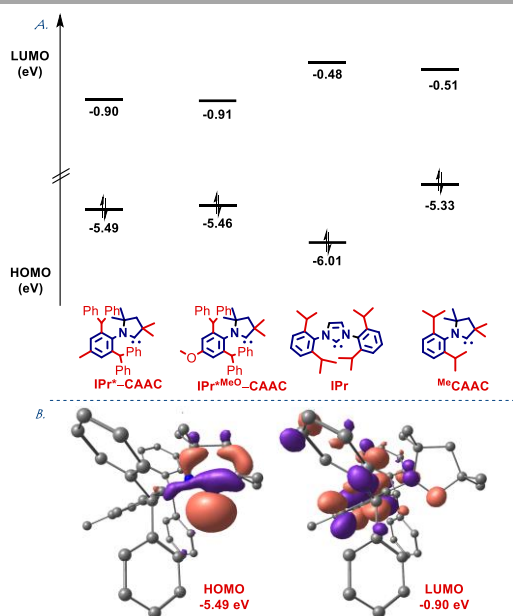


Figure 4. (A) HOMO and LUMO energy levels (eV). (B) HOMO (σ-donating orbital) and LUMO (π-accepting orbital) of IPr*-CAAC 5a. B3LYP 6-311++g(d,p) level. See SI.

In conclusion, we have developed a unique family of highly-hindered CAAC ligands derived from IPr*. These ligands represent a merger of highly hindered and sterically-flexible IPr* with strongly electron-rich, quaternary carbon-substituted CAACs. These novel characteristics and availability of various IPr* and CAAC templates offer a significant potential to expand the arsenal of NHC ligands to electron-rich bulky architectures with key applications in metal stabilization and catalysis. Future studies are directed toward the synthesis of chiral ligands and the expansion to other metal complexes.

We thank Rutgers University, the NIH (R35GM133326), the NSF (CAREER CHE-1650766). Supplement funding was provided by the Rutgers University Newark Chancellor's Research Office.

Notes and references

- 1 A. Meijere, de S. Bräse, M. Oestreich, *Metal-Catalyzed Cross-Coupling Reactions and More*, Wiley-VCH, Weinheim, Germany 2014.
- 2 C. C. C. Johansson Seechurn, M. O. Kitching, T. J. Colacot and V. Snieckus, *Angew. Chem., Int. Ed.* 2012, **51**, 5062.
- 3 A. J. Arduengo, R. L. Harlow and M. A. Kline, *J. Am. Chem. Soc.* 1991, **113**, 361-363.

- 4 W. A. Herrmann, M. Elison, J. Fischer, C. Kocher, and G. R. J. Artus, *Angew. Chem., Int. Ed.* 1995, **34**, 2371.
- 5 J. Huang and S. P. Nolan, *J. Am. Chem. Soc.* 1999, **121**, 9889.
- 6 (a) M. N. Hopkinson, C. Richter, M. Schedler and F. Glorius, *Nature* 2014, **510**, 485. (b) P. Bellotti, M. Koy, M. N. Hopkinson and F. Glorius, *Nat. Rev. Chem.* 2021, **5**, 711. (c) S. P. Nolan, *N-Heterocyclic Carbenes: Effective Tools for Organometallic Synthesis*, Wiley: Weinheim, 2014. (d) S. P. Nolan and C. S. J. Cazin, *Science of Synthesis: N-Heterocyclic Carbenes in Catalytic Organic Synthesis*, Thieme: Stuttgart, 2017. (e) H. V. Huynh, *The Organometallic Chemistry of N-Heterocyclic Carbenes*, Wiley: Hoboken, 2017.
- 7 V. Lavallo, Y. Canac, C. Präsang, B. Donnadieu and G. Bertrand, *Angew. Chem. Int. Ed.* 2005, **44**, 5705.
- 8 For non-classical and less heteroatom stabilized carbenes, see: (a) O. Schuster, L. R. Yang, H. G. Raubenheimer and M. Albrecht, *Chem. Rev.* 2009, **109**, 3445; (b) R. H. Crabtree, *Coord. Chem. Rev.* 2013, **257**, 755. (c) A. Vivancos, C. Segarra and M. Albrecht, *Chem. Rev.* 2018, **118**, 9493; (d) S. C. Sau, P. K. Hota, S. K. Mandal, M. Soleilhavoup and G. Bertrand, *Chem. Soc. Rev.* 2020, **49**, 1233; (e) W. C. Chen, W. C. Shih, T. Jurca, L. Zhao, D. M. Andrada, C. J. C. Chang, S. K. Liu, Y. P. Wang, Y. S. Wen, G. P. A. Yap, C. P. Hsu, G. Frenking and T. G. Ong, *J. Am. Chem. Soc.* 2017, **139**, 12830.
- 9 For reviews, see: (a) M. Melaimi, M. Soleilhavoup, and G. Bertrand, *Angew. Chem. Int. Ed.* 2010, **49**, 8810; (b) M. Soleilhavoup and G. Bertrand, *Acc. Chem. Res.* 2015, **48**, 256; (c) M. Melaimi, R. Jazzar, M. Soleilhavoup and G. Bertrand, *Angew. Chem. Int. Ed.* 2017, **56**, 10046; (d) Jazzar, R.; Soleilhavoup, M. and G. Bertrand, *Chem. Rev.* 2020, **120**, 4141. For selected examples, see: (e) L. Zhao, C. Hu, X. Cong, G. Deng, L. L. Liu, M. Luo and X. Zeng, *J. Am. Chem. Soc.* 2021, **143**, 1618. (f) S. Roy, K. C. Mondal and H. W. Roesky, *Acc. Chem. Res.* 2016, **49**, 357; (g) G. Wang, L. A. Freeman, D. A. Dickie, R. Mokrai, Z. Benkő and R. J. Gilliard Jr., *Chem. Eur. J.*, 2019, **25**, 4335.
- 10 (a) F. Izquierdo, S. Manzini and S. P. Nolan, *Chem. Commun.* 2014, **50**, 14926; (b) J. Diesel, A. M. Finogenova, N. Cramer, *J. Am. Chem. Soc.* 2018, **140**, 4489; (c) S. Okumura, S. Tang, T. Saito, K. Semba, S. Sakaki and Y. Nakao, *J. Am. Chem. Soc.* 2016, **138**, 14699; (d) N. I. Saper, A. Ohgi, D. W. Small, K. Semba, Y. Nakao and J. F. Hartwig, *Nat. Chem.* 2020, **12**, 276; (e) T. Carroll, D. E. Ryan, J. D. Erickson, R. M. Bullock and B. Tran, *J. Am. Chem. Soc.* 2022, **144**, 13865.
- 11 (a) N. Marion and S. P. Nolan, *Acc. Chem. Res.* 2008, **41**, 1440; (b) T. Scattolin and S. P. Nolan, *Trends Chem.* 2020, **2**, 721.
- 12 D. Martin, N. Lassauque, B. Donnadieu and G. Bertrand, *Angew. Chem. Int. Ed.* 2012, **51**, 6172.
- 13 S. Würtz and F. Glorius, *Acc. Chem. Res.* 2008, **41**, 1523.
- 14 G. Berthon-Gelloz, M. A. Siegler, A. L. Spek, B. Tinant, J. N. H. Reek and I. E. Markó, *Dalton Trans.* 2010, **39**, 1444.
- 15 For an excellent review, see: H. V. Huynh, *Chem. Rev.* 2018, **118**, 9457.
- 16 (a) S. Shi, S. P. Nolan, M. Szostak, *Acc. Chem. Res.* 2018, **51**, 2589; (b) Q. Xia, S. Shi, P. Gao, R. Lalancette, R. Szostak and M. Szostak, *J. Org. Chem.*, 2021, **86**, 15648; (c) T. Zhou, G. Li, S. P. Nolan and M. Szostak, *Org. Lett.*, 2019, **21**, 3304; (d) S. Yang, T. Zhou, A. Poater, L. Cavallo, S. P. Nolan and M. Szostak, *Catal. Sci. Technol.* 2021, **11**, 3189; (e) T. Zhou, S. Ma, F. Nahra, A. M. C. Obled, A. Poater, L. Cavallo, C. S. J. Cazin, S. P. Nolan and M. Szostak, *iScience*, 2020, **23**, 101377. (f) Q. Zhao, G. Meng, G. Li, C. Flach, R. Mendelsohn, R. Lalancette, R. Szostak, M. Szostak, *Chem. Sci.* 2021, **12**, 10583;
- 17 (a) A. A. Danopoulos, T. Simler and P. Braunstein, *Chem. Rev.* 2019, **119**, 3730; (b) Y. Gao, S. Yazdani, A. IV Kendrick, G. P. Junor, T. Kang, D. B. Grotjahn, G. Bertrand, R. Jazzar and K. M. Engle, *Angew. Chem. Int. Ed.* 2021, **60**, 19871;
- 18 (a) A. C. Hillier, W. J. Sommer, B. S. Yong, J. L. Petersen, L. Cavallo and S. P. Nolan, *Organometallics* 2003, **22**, 4322; (b) L. Falivene, Z. Cao, A. Petta, L. Serra, A. Poater, R. Oliva, V. Scarano, L. Cavallo, *Nat. Chem.* 2019, **11**, 872.
- 19 S. V. C. Vummaleti, D. J. Nelson, A. Poater, A. Gomez-Suarez, D. B. Cordes, A. Slawin, S. P. Nolan and L. Cavallo, *Chem. Sci.* 2015, **6**, 1895.
- 20 G. Meng, L. Kakalis, S. P. Nolan, M. Szostak, *Tetrahedron Lett.* 2019, **60**, 378.